GRANT
IN-59-CR
329086
P30

SEMI-ANNUAL PROGRESS REPORT
NAG8-708-5

HIGH TEMPERATURE FURNACE MODELING AND PERFORMANCE VERIFICATIONS

Submitted to

Richard M. Poorman

Mail Code JA62
George C. Marshall Space Flight Center
National Aeronautics and Space Administration
Huntsville, Alabama 35812

Prepared by

James E. Smith, Jr., Ph.D.

Chairman and Associate Professor
Department of Chemical Engineering
College of Engineering
The University of Alabama in Huntsville
Huntsville, Alabama 35899

January 1991

Table of Contents

ABSTRACT

A two dimensional conduction/radiation problem for an alumina crucible in a zirconia heater/muffle tube enclosing a liquid iron sample was solved numerically. Variations in the crucible wall thickness were numerically examined. The results showed that the temperature profiles within the liquid iron sample were significantly affected by the crucible wall thicknesses.

New zirconia heating elements are under development that will permit continued experimental investigations of the zirconia furnace. These elements have been designed to work with the existing furnace and have been shown to have longer lifetimes than commercially available zirconia heating elements. The first element has been constructed and tested successfully.

1.0 INTRODUCTION

Under NASA Grant NAG8-708 we are performing analytical, numerical, and experimental studies on two classes of high temperature materials processing furnaces. The research concentrates on a commercially available high temperature furnace using zirconia as the heating element and an Arc Furnace under design at NASA's MSFC, based on a ST International tube welder.

1.1 Objectives

There were two major objectives during this reporting period. The first objective was to expand the one dimensional numerical model to a two dimensional radiation/conduction model. Two dimensional interactions between the zirconia heater/muffle tube and the alumina ampule were included in this model to resolve the problems which occurred while using the one-dimensional model. The second objective was to design and construct new zirconia heating elements. The method of construction was very similar to that which was suggested in our previous progress report. The zirconia element was designed to address problems which were discovered using two commercially available elements. As explained in previous reports, the commercially available elements developed cracks in relatively short periods, thus hindering the development of the zirconia furnace for materials processing.

1.1.1 Objective 1. Two Dimensional Numerical Model

The one dimensional model developed to estimate the thermal profiles within an alumina crucible, having semitransparent radiation properties, was found to be insufficient to study the effects of variations in crucible wall thicknesses. Variations of temperature profiles within the crucible wall are required to determine the optimum crucible wall thickness for samples containing molten iron.

To solve this problem, a two-dimensional model was developed to improve the overall understanding of heat transfer interactions occurring within the zirconia furnace. The two-dimensional analysis more closely models both the spectral radiation and conduction occurring within the zirconia furnace. Using the two-dimensional model, temperature profiles within the crucible wall and the liquid iron sample were determined. The knowledge of the temperature profiles is important in the design of this furnace, since, as will be shown, the location of the maximum in the temperature profile was a function of the crucible wall thickness.

An important requirement in the design of an efficient furnace is that the maximum temperature location be at a minimum distance from the crucible/liquid iron interface, resulting in higher temperatures within the sample. If the maximum temperature within the crucible wall occurs near the crucible/liquid iron interface then the crucible wall can basically be neglected

during control of the zirconia furnace. A detailed discussion of the theoretical and numerical work performed on the two-dimensional model are provided in section 2.

1.1.2 Objective 2. Zirconia Furnace Heating Elements

The zirconia heating elements for which the design was suggested in the previous progress report, have been received. The platinum/rhodium wire and platinum ink were also received. We have completed the construction of one element, which to date has operated for over 20 hours without signs of defects. This element is still receiving study. The furnace has now been modified to permit both current and voltage measurements to be made and recorded. This provides a measure of the applied power as a function of the element's operating time at a fixed applied voltage.

In the following sections, a detailed development of the two dimensional furnace model and a description of the furnace element construction are presented.

2.0 TWO DIMENSIONAL MODEL

In the following sections detailed discussions of the theory and numerical analysis of the spectral radiation and conduction models are presented.

2.1 Literature Survey

Chang and Smith [1] analyzed the heat transfer in a conducting, emitting and absorbing medium bounded by two infinite coaxial cylindrical surfaces, for both transient and steady states. They formulated the problem in two differential equations (one for the radiation potential and the other for the temperature) using quasi-steady simplification and eddington's first approximation for radiative transfer. They found that for highly emissive surfaces, the interaction of radiation with conduction has a negligible effect on the total heat flux. Ho and Ozisik [2] used the Galerkin method to obtain an exact solution to the radiation part of the problem, and a finite-difference scheme to solve the conduction part. They solved a steady-state conduction and radiation heat transfer for an absorbing, emitting and isotropically scattering two dimensional rectangular enclosure. They examined the effects of the conduction-to-radiation parameter, the single scattering albedo, and the aspect ratio on the temperature distribution. They considered the boundary surfaces to be black and subjected to a constant temperature on one surface and zero temperature on others.

A modified finite difference approach to the problem of transient combined conduction and radiation in an absorbing and emitting annular medium was presented by Gordaninejad and Francis [3] in 1984. They studied two different boundary conditions; the

first one was a step change in temperature on both inner and outer surfaces, while the second type of boundary condition was a step flux in the inner surface. The solution was shown to closely represent the exact solution for the case of pure conduction. Fernandes and Francis [4] solved a transient combined conduction and radiation in a gray absorbing, emitting, and scattering medium of cylindrical geometry, using the Galerkin finite element method. The results were compared with exact solutions for the extreme cases, i.e., pure conduction and radiative equilibrium.

In this study we have considered all the radiative properties, namely transmissivity, absorptivity, and emissivity as functions of both wavelengths and temperatures. This is important since at such high temperatures (1500 - 2000^{o}C) the radiation properties vary due the transparency of the ceramics. The transparency of ceramics at these temperatures is an important advance in the high temperature modeling of ceramics and must be understood if we are to advance high temperature furnace technology.

2.2 Physical Model

The model considered here is shown in figure 1. A muffle tube/heating element, hereto referred as the heating element, encloses an alumina crucible wall containing a liquid iron sample. The heating element, made of yttrium stabilized zirconia, acts as an isothermal radiant source of energy. The alumina

crucible will be considered opaque for certain frequencies of radiation and semitransparent for other regions of the radiation spectrum. Heat will be transmitted through the crucible wall by radiation and conduction, while in the liquid iron sample conduction is considered as the main mode of energy transfer. The effects of the spectral radiation to conduction parameters on the temperature profiles in the crucible wall were presented in previous reports, which showed that radiation is the dominating factor in the energy transfer within the alumina crucible wall at these temperature ranges.

Spectral radiant energy will be transferred from the zirconia heating element radially into the alumina crucible wall through a vacuum. The energy will further be transferred into the liquid metal radially and in the axial direction. The cooling of the liquid iron sample is encountered at both ends of the sample, that is at the top and bottom of the liquid iron sample. Therefore the heat flux at both ends is equivalent.

As shown in figure 1, region I is a vacuum between the zirconia heating element and the alumina crucible wall. Region II is the crucible wall made of alumina. In this region both radiation and conduction are assumed to take place. Region III is the liquid iron sample. In this region conduction will be considered as the major source of heat transfer.

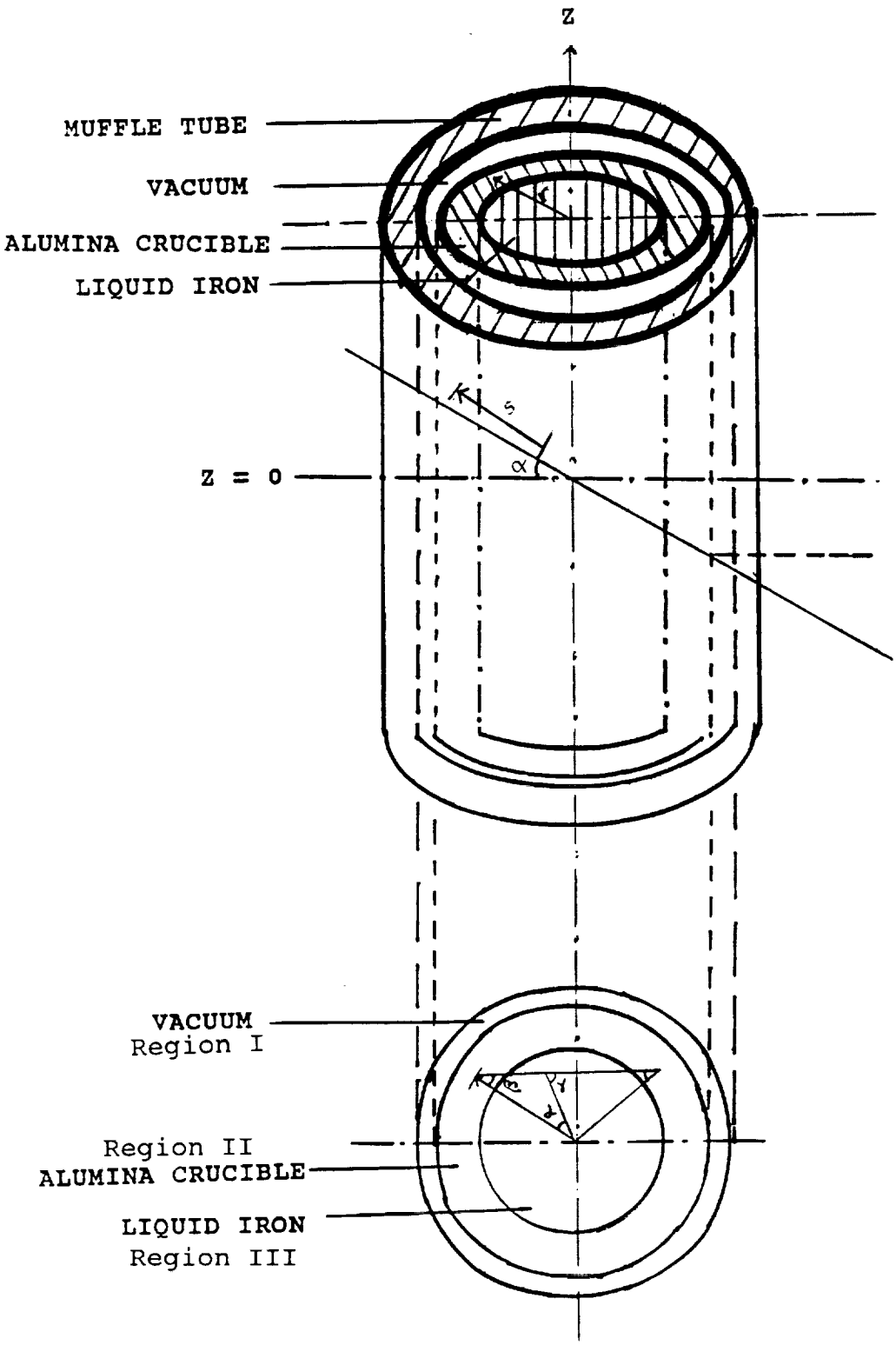

Figure 1. An outline of the alumina crucible containing liquid iron and enclosed by a heated furnace wall.

2.2.1 Physical Properties

As in the one dimensional study, the radiation properties, namely absorptivity, emissivity, and transmissivity are considered as functions of temperature and wavelength. The thermal conductivities for the alumina crucible and the liquid iron sample are also functions of temperature. These functions have been described in detail in the previous progress report.

2.2.2 Analysis

At steady state in the absence of internal heat sources, conservation of energy requires that

$$-\nabla \cdot (\nabla T) + \nabla \cdot Q_R = 0 \qquad (1)$$

be satisfied. This implies that the sum of the conductive and radiative fluxes must equal the total heat flux. For an annular geometry with cylindrical symmetry, equation (1) in cylindrical coordinates becomes

$$-[1/r \; \partial/\partial r(k \; \partial T/\partial r)] - \partial/\partial z(k \; \partial T/\partial z) + \partial Q_R/\partial r + Q_R/r = 0 \qquad (2)$$

where the first two terms represent conduction in the radial and axial directions respectively. The second term represents the radiation in the radial direction. Note that radiation is assumed

negligible in the axial direction, within the crucible wall. Also in the liquid iron, only conduction is considered to be the dominating mode of heat transfer.

Using dimensionless variables defined as follows

$$\tau = \int_0^{\infty} \kappa_\lambda r d\lambda \tag{3}$$

$$\theta = T/T_{ref} \tag{4}$$

$$\eta = z/z_0 \tag{5}$$

equation (2) becomes

$$\frac{1}{\tau}\frac{\partial}{\partial \tau}\left(k\frac{\partial \theta}{\partial \tau}\right) + \frac{1}{\kappa^3 z^2_0}\frac{\partial}{\partial \eta}\left(\frac{\partial \theta}{\partial \eta}\right) = \frac{1}{N}\frac{\partial Q_R(\tau)}{\partial \tau} + \frac{Q_R(\tau)}{\tau} \tag{6}$$

where we define the radiation conduction parameter N as follows

$$N = \kappa^2/4\sigma_s T^3_{ref} \tag{7}$$

The transport equation, using the coordinates shown in figure 1 for a material with refractive index, n, is given by

$$dI_\lambda/d\tau = -\beta_\lambda I_\lambda + \kappa_\lambda n^2 I_{b\lambda} + \sigma_\lambda G_\lambda(r)/4\pi \tag{8}$$

where I_λ, the intensity and is composed of I^+ and I^- which are dependent on the direction of radiation, and $G_\lambda(r)$ is the integrated intensity defined below.

$$G_\lambda(r) = 2\int_0^{\pi/2}\int_0^{2\pi} I_\lambda \cos\alpha \, d\gamma \, d\alpha \tag{9}$$

Therefore, the net radiative flux directed radially inward is given by

$$q_\lambda(r) = 2\int_0^{\pi/2}\int_0^{2\pi} I_\lambda \cos^2\alpha \cos\gamma \, d\gamma \, d\alpha \tag{10}$$

From the above equation (10), the expression for the radiative flux directed inward in nondimensionless form is

$$Q_R(\tau) = 4\tau_1/\pi\tau \int_0^{\pi/2}\int_0^{\sin^{-1}(\tau_0/\tau_1)} \{ \Phi_1^+(\tau,\alpha,\beta) - \Phi_1^-(\tau,\alpha,\beta) \} \cos^2 \cos\beta \, d\beta \, d\alpha$$

$$+ 4\tau_1/\pi\tau \int_0^{\pi/2}\int_{\sin^{-1}(\tau_0/\tau_1)}^{\sin^{-1}(\tau/\tau_1)} \{ \Phi_2^+(\tau,\alpha,\beta) - \Phi_2^-(\tau,\alpha,\beta) \} = \cos^2\alpha \cos\beta \, d\beta \, d\alpha \tag{11}$$

where Φ is the nondimensionalized radiation potential defined as

$$\Phi = \pi I / n^2 \sigma_s T^4_{ref}$$

and I is the intensity of radiation.

Substituting equation (11) into equation (6) gives the final form of the governing equation.

2.2.3 Boundary Conditions

We will basically consider two kinds of boundary conditions. First, case (1), we shall assume that the surface of the crucible is opaque. Secondly, case (2), this same surface will be considered as semitransparent for some regions of radiation wavelengths. The other boundary condition for both cases (1) and (2) will be a net zero heat flux at the center of the liquid iron sample. This assumption is justified by the cylindrical symmetry of the model.

Since the model now has two separate regions where heat transfer is being considered, that is region II and III, there exists another restriction at the interface of the crucible wall and the liquid iron sample. At this interface between the crucible and the liquid iron sample, we shall assume that the temperature is continuous, thus the heat fluxes on both sides will be identically matched. This assumption is justified by the fact that the crucible wall and the liquid iron sample are in thermal contact therefore the temperatures at both sides of the interface are equal.

For case (1), the opaque case, the temperature at the crucible wall surface will be calculated from the radiating zirconia element. This implies that at the boundary $\eta = 0$ will be fixed at a known temperature. For the semitransparent case (2), the boundary condition at the surface of the wall is given below

$$-K\partial\theta/\partial\tau\Big|_{\tau=R} + \epsilon_{opq}[e_{b\lambda opq}(T_1) - e_{b\lambda opq}(T_0)] = 0 \qquad (12)$$

When we consider the interface, as mentioned earlier, the temperatures at the crucible side and the temperature on the liquid iron side have to be identical. Therefore we can write

$$T_{crucible} = T_{iron} \quad \text{at} \quad T = T_{interface} \qquad (13)$$

For both cases (1) and (2), that is opaque and transparent cases respectively, the boundary condition at the center of the liquid metal sample is that the temperature gradient is zero. Thus we have

$$d\theta/d\tau = 0 \qquad (14)$$

Now for the iron sample we have two more boundary conditions for the axial (z) direction. According to the coordinate system applied to the model (see figure (1)), at the center of the sample, ($\eta = 0$), we have

$$d\theta/d\eta = 0 \qquad (15)$$

while at each end of the crucible wall ($\eta = 1,-1$), we have

$$d\theta/d\eta = 0.5Q_R \tag{16a}$$

$$d\theta/d\eta = -0.5Q_R \tag{16b}$$

Equations (6) and (11) together with the boundary conditions are the final equations needed to solve the problem.

2.3 Numerical Formulation

A finite difference formulation of the energy equation (6) is given by [A] [θ] = [radiation terms]. The coefficient matrix [A] consists of the following

$$a_{n-1,m} = k_{n-1/2}/g^2\tau_m$$

$$a_{n,m} = (-k_{n+1/2} - k_{n-1/2})/g^2\tau_m + (k_{n+1/2} - k_{n-1/2})/h^2\kappa^3z^2{}_0$$

$$a_{n+1,m} = k_{n+1/2}/g^2\tau_m$$

$$a_{n,m-1} = -k_{n-1/2}\ /h^2\kappa^3z^2{}_0$$

$$a_{n,m+1} = k_{n+1/2}\ /h^2\kappa^3z^2{}_0$$

where $k_{n+1/2}$ is defined as $0.5(k_n + k_{n+1})$ and $k_{n-1/2}$ is defined as $0.5(k_{n-1} + k_n)$ with being the thermal conductivity at temperature θ_n and where $g = \Delta\tau$ and $h = \Delta\eta$.

The left hand side coefficient matrix represents the conduction terms, while the right hand side represents the integral radiation terms. The finite difference equations for the conduction part included two spatial variables, namely r and η in the radial and axial directions respectively. For the crucible wall, the integrals on the right hand side of equation (6) were calculated in the following manner. For an assumed temperature , the integrals were calculated using simpson's method for the range of wavelengths given between each of the nodes. This provided the total radiation properties at those nodes. Since this problems represents a double integration of complex mathematics, simpson's rule was used to integrate over discrete wavelengths to reduce the problem to a single integral of sums of the integrated wavelengths, which were further integrated using a three point gaussian quadrature. This calculation provided the elements for the force vector at each of the nodes. For this force vector the temperature was assumed linear between the nodes.

The coefficient matrix for the crucible calculations was only in terms of radial steps $\Delta\eta$, while the coefficient matrix of the liquid iron calculations were in two spatial directions, that is in the radial and axial directions. The implicit method was used to solve the equations in region II (the crucible wall), and the flux and temperature leaving the end node of the wall was used to start the calculations in region III (the iron sample).

When both the solutions converged, a test was performed to compare the fluxes at the interface. When the thermal fluxes were within the prescribed error of 10^{-2} the profiles were assumed to converge.

3.0 EXPERIMENTS AND PROCEDURES

The construction and assembly of the zirconia heating elements will be discussed in section 3.1. The design of the zirconia elements used results from our numerical studies, various theoretical considerations, and experimental results obtained from previous data on similar heating elements.

3.1 Construction and Assembly of Heating Elements

The zirconia heater elements were ordered and received from McDanel Refractory Company. The elements were 4.5 inches in length, and contained platinum bands (0.25 inches wide) at distances 0.25 inches from the ends.

The platinum/rhodium (10%) wire, 1000 feet in length and 0.003 inches in diameter, was ordered and received from Englehard Corporation. The wire was then cut into 80 2-ft. strands and twisted to form the lead wires for the zirconia heating element. The number of strands needed was calculated based on the current loads expected during the operation of the furnace. The length of the lead wires were established to accommodate the construction of about five additional heater elements. The lead wires can be

reused to construct other elements by cutting off the portion that was attached to the used zirconia heating element, thus resulting in a decreased construction cost per element.

The wires were attached to the zirconia heating element to form a current carrying junction between the zirconia heater element and the lead wires using a special approach. The junction was then cured several times using a Watlow furnace. The temperature was increased at a rate of 5^{o}C per minute to 225^{o}C and held at that temperature for another hour. This operation ensured that trapped gases would diffuse out of the junction. The temperature was then raised to 525^{o}C at the rate of 5^{o}C per minute and held there for about one hour. At this stage all the gases and moisture were removed. The temperature was raised to 1025^{o}C and held for another hour. The power was removed from this well insulated furnace and the system allowed to cool undisturbed over night.

3.2 Experimental Procedures

The zirconia heater element was then installed into the ARTCOR furnace body following their procedures. Their control system was reconfigured and programmed to operate at a maximum of 70% applied power. The variables for preheater power, ramping times and rates, and other related variables were adjusted as suggested by the manufacturer.

For the initial run, the preheater power was set at 43% for 0.7 hr. A successful run was accomplished. The element reached its conduction temperature, referred to here as ignition, and was held at that power setting (70%) for an hour.

After the first run, the controller would not function. We contacted the manufacturer of the controller (Eurotherm) and were advised that the cpu and ram chips would require upgrading. This problem would have required substantial modification of the controller by the manufacturer and unexpected costs. It was decided to devise a method to bypass the controller and continue uninterrupted study of the newly prepared element.

The method devised required two independent power sources. One source would heat and control the preheater, while the other source would supply the power to the zirconia heating element once the ignition temperature had been reached.

A Valley Forge linear programmer was used to control power to the preheater. This controller ramps the preheater voltage based on a temperature measurement from a type K thermocouple. This thermocouple was inserted between the preheater and zirconia heating element and was removed once the zirconia ignition temperature was achieved.

The zirconia main heater was connected to a variable transformer through a current meter. The variable transformer was calibrated using a voltmeter and manually operated during the experimental procedures.

In operation, once the preheat temperature of the zirconia element reached its conduction temperature, the variable transformer voltage was initially set to 120 VAC while monitoring the current flowing in the element. Once the current increased to about 3 amps at 120 VAC, power to the preheater was switched off and the thermocouple removed. The voltage from the transformer was then gradually reduced to a constant operating voltage. Current within the zirconia main heater was monitored for several hours at the constant applied voltage until equilibrium was achieved. This procedure ensures that the main heating element ignites prior to disconnecting the preheater power as it does with the manufacturer control scheme.

Cooling was accomplished by gradually reducing the voltage applied to the zirconia element until current no longer flowed in the element. This protects the element from rapid cooling which may induce thermal stresses within the element.

4.0 RESULTS AND DISCUSSION

4.1 OBJECTIVE 1. Two-Dimensional Numerical Model

One of the main objectives of the two-dimensional analysis was to examine the effect of the variation in temperature profiles within crucible walls of varying thickness, with the heating element at a constant temperature of 1600^{o}C. The results are shown in figure 2 for different values on N (the radiation-

conduction parameter). Here N is proportional to the ratio of crucible to liquid iron thicknesses, namely 1:3, 1:1, and 4:1. Therefore the variations in temperature profiles are as a result of the total heat capacities of the crucibles and the heat dissipation in the axial direction within the liquid iron sample.

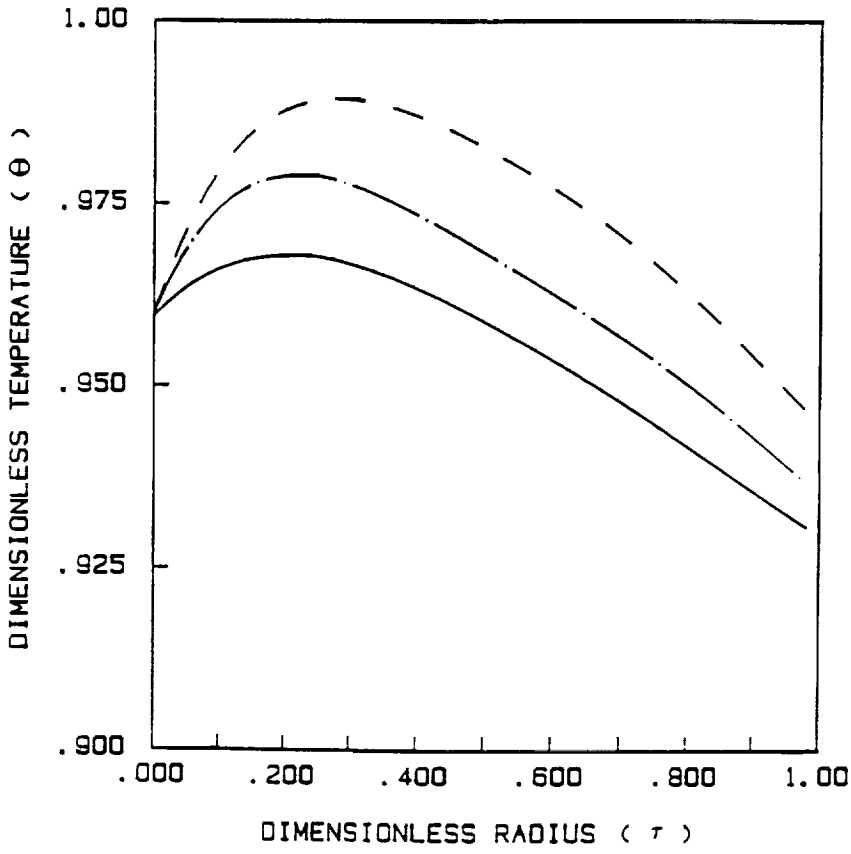

Figure 2. Variation of dimensionless temperature with radial distance for varying crucible thicknesses. (- - -) is for 1:3, (-·-) is for 1:1, (——) is for 4:1 ratio for crucible to iron sample.

Since heat is dissipated from both the top and bottom of the sample, the temperature profiles towards these ends will be more pronounced than the profiles within the center of the model.

When the relative thicknesses for the alumina crucible and the liquid iron samples are the same (see figure (3)) it was noticed that conduction in the liquid iron (region III) is strongly influenced by the thermal profile developed within the crucible wall.

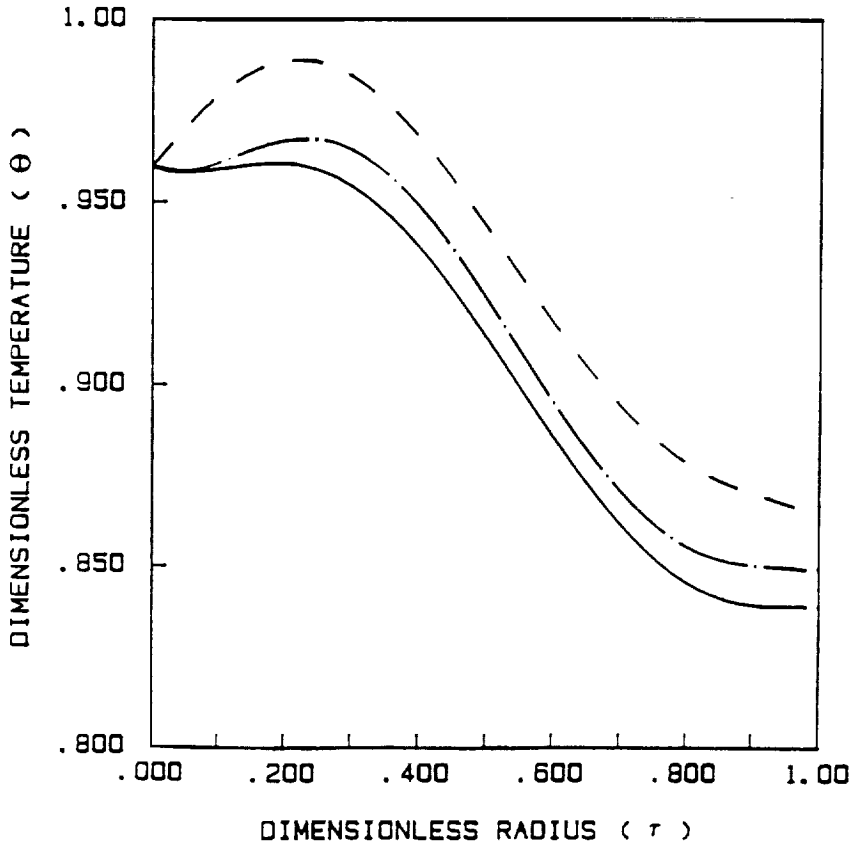

Figure 3. Variation of dimensionless temperature with radial distance for varying distances in the r direction. (- - -) is for r=0.75, (-·-) is for r=0.5, (——) is for r=0.25. Ratio of crucible to iron is 1:1.

Notice that as the crucible wall gets thinner, the thermal profile increases to a maximum almost at the liquid iron interface. This suggests that an optical pyrometer observing the crucible wall would be largely measuring the temperature of the liquid iron surface.

In figure (4), the ratio of the crucible wall thickness to that of the iron sample is 1:3.

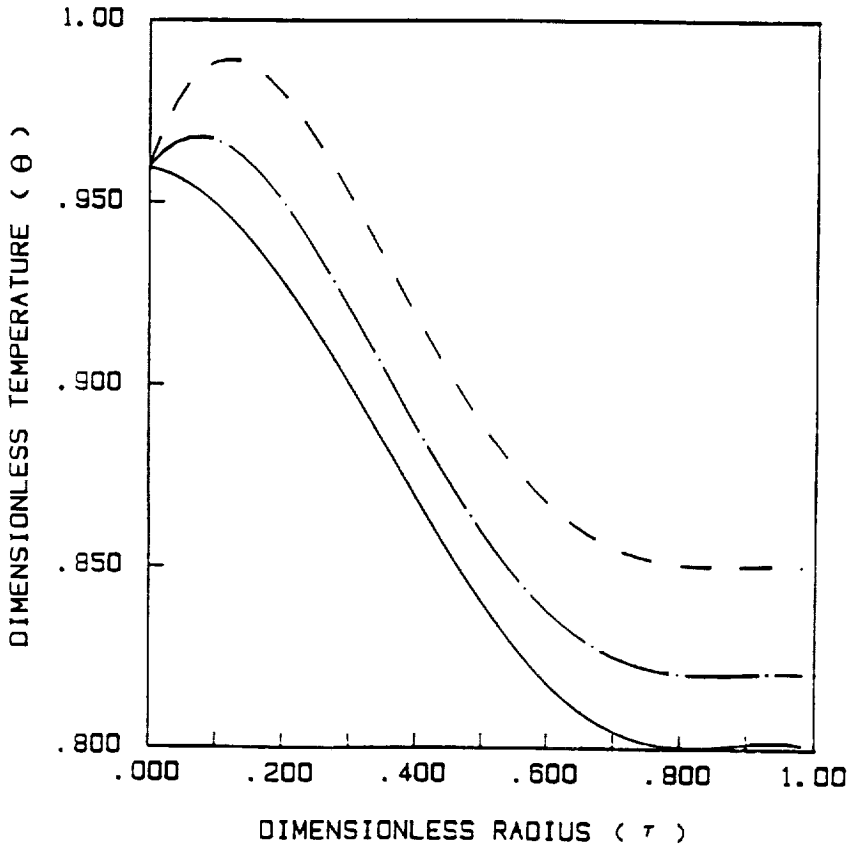

Figure 4. Variation of dimensionless temperature with radial distance for varying distances in the τ direction. (- - -) is for τ=0.75, (-•-) is for τ=0.5, (——) is for τ=0.25. Ratio of crucible to iron is 1:3.

The temperature at the crucible/iron interface is shown to be much greater than for the previous cases. This is desirable since for a given power to the furnace, one would like to achieve a high temperature at the liquid iron interface while ignoring the crucible wall. This means that the radiative effects within the crucible are minimized with respect to the bulk sample.

4.2 Objective 2. Zirconia Furnace Heating Elements

The experimental runs were designed to study several aspects of the new zirconia heating elements. Figure (4) show the results of one of these experiment. In this figure is shown the current history from the element operated at a constant voltage of 98 VAC. Notice that the current rises as a function of time due to the fact that as the element heats its resistance continually decreases from about 445 ohms to a final resistance of 21.2 ohms. This corresponds to a current of 4.62 amps after about 1 1/2 hours of operation. At this writing, the new zirconia element has operated for over 20 hours. Previously reported results on the two commercially available elements showed that they operated for 3 and 15 hours before failure. The commercial elements carried a measured maximum current of 4.6 amps, while the new element was found to carry currents of over 7 amperes.

During initial operation, we noticed that if the preheater was shut off before ignition of the main heater element, convection through the bore of the element, cooled ends of the

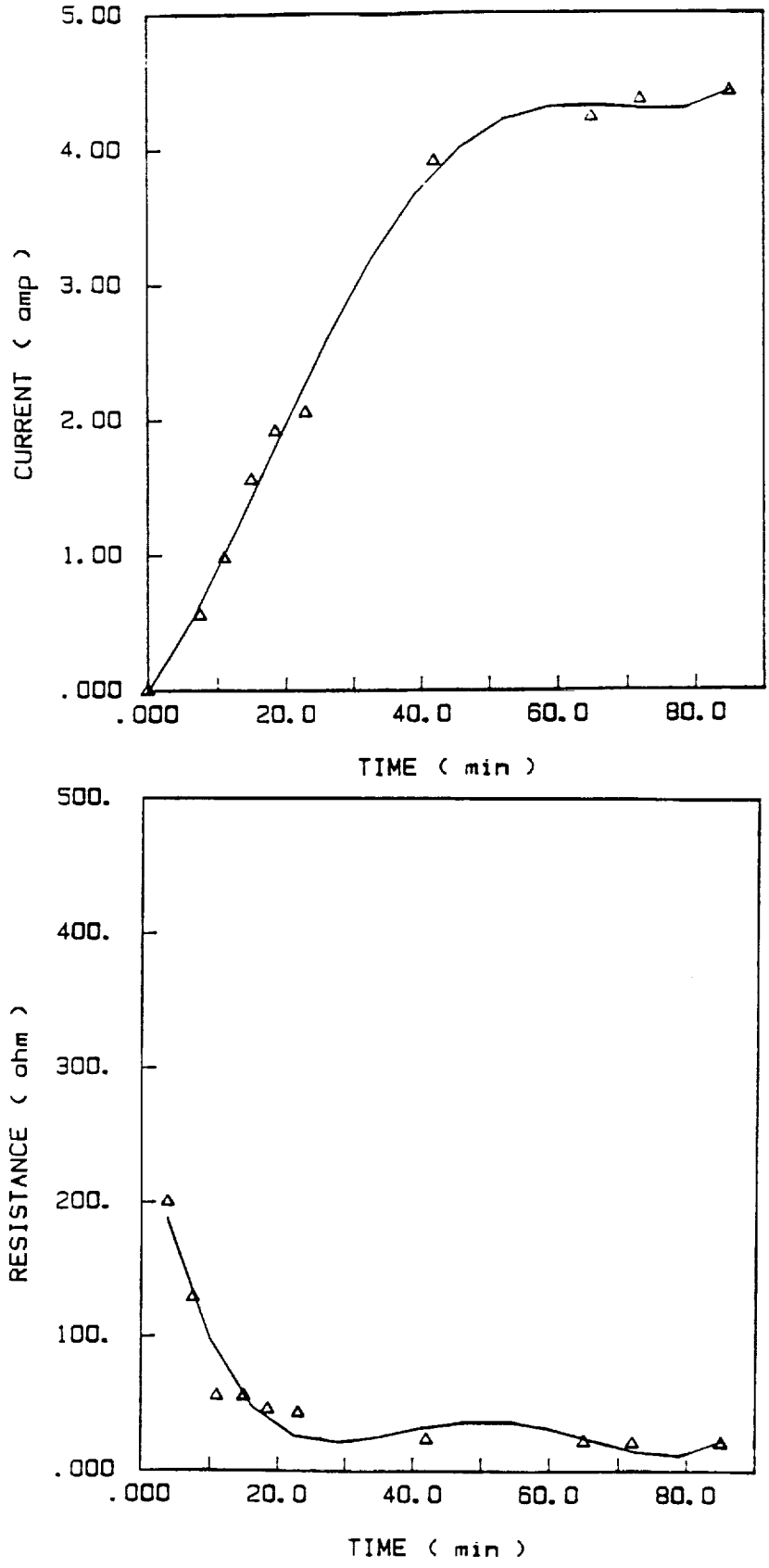

Figure 5. Variation of current (top) and resistance (bottom) with time for a constant voltage of 98 VAC.

heating elements at the points where the wires were attached. This creates a higher resistance and thus prevents the ignition of the element. Higher currents measured in the new element may result from techniques used to attach the lead wires.

5.0 CONCLUSIONS

The two dimensional model proved to be very successful in accurately modeling the furnace. The results have provided a greater detailed understanding of the components of this advanced high temperature furnace.

The parametric study of the ratio of the crucible wall to the liquid iron sample, has shown that there is a significant increase in the temperature at the interface (between the liquid iron sample and the crucible wall) with decreasing crucible thickness. Also, the radiation effects on the sample are greatly reduced for thin crucible walls. This allows a greater portion of the iron sample to attain a uniform radial temperature profile. For a thick wall, an optical pyrometer would measure an average temperature of wall. Optical pyrometer measurements for a thin wall would virtually be measuring the interfacial temperature at the liquid iron sample. The general conclusion from this portion of the study is to select as thin a crucible as will tolerate the loads applied during processing.

We have shown the initial performance to date for a new zirconia element design and initial indication show consistent performance and greater power handling capabilities.

6.0 FUTURE WORK

We intend to assemble several zirconia elements and test them for sensitivity to water vapor. We also intend to design the procedures and equipment needed to measure the centerline temperature of the furnace using a thermocouple and a pure iron sample that will be melted within the furnace. The data obtained from the furnace measurements will be compared to those predicted by the two dimensional model that has been completed.

NOMENCLATURE

τ_λ = optical thickness

τ = dimensionless distance in the radial direction (eqn. 3)

η = dimensionless distance in the z direction (z/z_0)

k = thermal conductivity

ϵ = emmissivity

κ = absorptivity

n = refractive index

σ = Boltzmann constant

$e_{b\lambda}$ = Planck's function

μ = $\cos\theta$

Θ = dimensionless temperature (T/T_{ref})

T = temperature (K)

Q_R = radiation heat flux

q_λ = radiative flux (eqn. 10)

I_λ = time rate of radiant energy per unit solid angle and per unit area normal to the radiant rays

K_λ = monochromatic absorption coefficient

E_n = exponential integral function

Φ_i = radiation potential (eqn. 11)

$B_{n\lambda}$ = radiosity defined in equation (12)

Subscripts

R = radiation

opq = opaque case

λ = monochromatic property

1,2 = indicate directions

+,- = positive and negative directions respectively

7.0 REFERENCES

[1] Chang, Yan-Po and Smith, Scott Jr., Int. J. Heat Mass Transfer vol. 13, pp. 69-80, 1970.

[2] Ho, C.H. and Ozisik, M.N., Numerical Heat Transfer, vol 13, n 2, March 1988 pp 229-239

[3] Gordaninejad, F. and Francis, J., Journal of Heat Transfer, Transactions ASME vol 106, n 4 Nov 1984 pp 888-891.

[4] Fernandes, R. and Francis, J., Journal of Heat Transfer, Transactions ASME vol 104 n 4 Nov 1982 pp 594-601.